Indonesian J. Pharm. Vol. 24 No 2 : 75 – 85
ISSN-p : 0126-1037

Research Article

CONSTRUCTION OF *IN SILICO* STRUCTURE-BASED SCREENING TOOLS TO STUDY THE OXIDATIVE METABOLITES FORMATION OF CURCUMIN BY HUMAN CYTOCHROME 450 3A4

Dewi Setyaningsih[1], Muhammad Radifar[2], Yosi Bayu Murti[3], Enade Perdana Istyastono[1,*]

[1]Pharmaceutical Technology Lab., Faculty of Pharmacy, Sanata Dharma University, Yogyakarta, Indonesia 55284.
[2]Graduate School of Biotechnology, Gadjah Mada University, Yogyakarta, Indonesia 55281.
[3]Pharmaceutical Biology Lab., Faculty of Pharmacy, Gadjah Mada University, Yogyakarta. Indonesia 55281.

Submitted: 24-09-2012
Revised: 12-10-2012
Accepted: 01-12-2012

*Corresponding author
Enade Perdana Istyastono

Email:
enade@usd.ac.id

ABSTRACT

Cytochrome P450 3A4 (CYP3A4) is a phase 1 metabolism enzyme which is responsible for the metabolism of about 30-40% drug in the market. This CYP3A4 is the most abundant CYP450 expressed in human body and also the one who is responsible for the biotransformation of most drugs. The competitive inhibition of curcumin (a yellow bioactive pigment discovered in *Curcuma sp.*) towards human CYP3A4 indicates that curcumin can be a substrate for the enzyme. In this study, *in silico* approaches employing molecular docking and interaction fingerprinting were used to predict the binding mode and the site of metabolism (SOM) of curcumin. Together with the SOMs retrieved previously and the list of possible reactions catalyzed by CYP3A4, the docking and fingerprinting results indicate that the most probable metabolite of curcumin metabolism by human CYP3A4 is an oxidative metabolite 1-(3,4-dihydroxyphenyl)-5-hydroxy-7-(4-hydroxy-3-methoxy-phenyl)hepta-1,4,6-trien-3-one.

Key words: site of metabolism (SOM), curcumin, biotransformation, *in silico*, molecular docking, protein-ligand interaction fingerprinting

INTRODUCTION

Cytochrome P450 3A4 (CYP3A4) is a part of the large protein family responsible in the phase 1 metabolism Cytochrome P450 (CYP450). This CYP3A4 is the most abundant CYP450 expressed in human body and also the one who is responsible for the biotransformation of most drugs available in the market (Rendic, 2002). The biotransformation catalyzed by this enzyme, including oxidation, hydroxylation, and heteroalkyl removal, depends on the binding mode and the reactivity of specific moiety of the drug (Rendic, 2002; Appiah-Opong *et al.*, 2008). This enzyme plays an important role in the drug-medicinal plants interactions (Appiah-Opong *et al.*, 2008; Appiah-Opong *et al.*, 2008). This indicates the probabilities of some bioactive compounds in the plants that serve as inhibitor or substrate for CYP3A4. Interestingly, the studies on CYP3A4 performed by Appiah-Opong *et al.* (2008) employed human CYP3A4 instead of animal models since the species differences could be detrimental for the conclusion drawing of the efficacy and safety potency of drug candidates (Komura and Iwaki, 2011).

The metabolism of curcumin (the yellow bioactive pigment discovered in *Curcuma sp.* (Kunwar *et al.*, 2008; Basnet and Skalko-Basnet, 2011)) by CYP3A4 is of considerable of interest (Asai and Miyazawa, 2000; Ireson *et al.*, 2001; Hoehle *et al.*, 2006; Anand *et al.*, 2007; Tamvakopoulos *et al.*, 2007; Appiah-Opong *et al.*, 2008). However, the fate of curcumin inside human body remains vague (Appiah-Opong *et al.*, 2007; Appiah-Opong *et al.*, 2008). Most clues about the fate of curcumin were collected from *in vitro* and *in vivo* studies using animal models (Asai and Miyazawa, 2000; Ireson *et al.*, 2001; Hoehle *et al.*, 2006; Anand *et al.*, 2007; Tamvakopoulos *et al.*, 2007). Fortunately, there were clear evidences shown that curcumin inhibits human CYP450 enzymes (*i.e.* CYP1A2, CYP2B6, and CYP3A4) in a competitive manner (Appiah-Opong *et al.*, 2007; Appiah-

Opong *et al*., 2008). Notably, amongst other tested human CYP450 enzymes, curcumin shows the highest inhibitory activity towards human CYP3A4 (Appiah-Opong *et al*., 2007). Hence, it is certain that curcumin binds to the active site of human CYP3A4 and probably acts as a substrate for the enzyme.

Several studies have shown that *in silico* methods can predict the potential susceptibility of a substrate towards certain CYP450 enzymes. An integrated *in silico* study even capable to predict the possible metabolites produced by CYP450 (de Graaf *et al*., 2005, 2006). Especially for CYP450 2D6 (CYP2D6), de Graaf *et al*. (2006) have constructed *in silico* structure-based virtual screening protocols to predict the site of metabolism (SOM) of substrates accurately and based on the SOM one could subsequently suggest the possible metabolites. On the other hand, computer-aided quantitative structure-activity relationship (QSAR) studies on curcumin and its analogs as inhibitors for several human CYP450, including CYP3A4 have been performed (Appiah-Opong *et al*., 2008). The QSAR studies suggested a statistically significant QSAR model on curcumin analogs as CYP3A4 inhibitor (Appiah-Opong *et al*., 2008). However, though the QSAR approaches successfully presented the prominent role of *in silico* methods in the studies of curcumin-CYP3A4 interaction (Appiah-Opong *et al*., 2008), the binding pose of curcumin in the CYP3A4 active pocket remains unclear. Notably, the broad selectivity of CYP3A4 (Rendic, 2002) and the inhibitory activity of curcumin towards this enzyme (Appiah-Opong *et al*., 2007; Appiah-Opong *et al*., 2008) make this enzyme worth to consider as the enzyme responsible for curcumin biotransformation. The availability of the crystal structure of human CYP3A4 (Sevrioukova and Poulos, 2012) offers the opportunities to predict the interaction between curcumin and CYP3A4 using *in silico* structure-based approaches. These approaches have the advantage of giving the insight of protein-ligand interaction (de Graaf *et al*., 2005). The structure-based approaches can hopefully show which moiety of curcumin that interacts with the CYP3A4 heme Fe-atom. Therefore, these approaches can be used to define the potential SOM of curcumin metabolized CYP3A4.

The research presented in this paper was aimed to elucidate the binding mode of curcumin in the CYP3A4 active site using valid *in silico* structure-based protocols and subsequently predict the SOM and the probable metabolite of curcumin by inspecting visually the curcumin-CYP3A4 interaction. Initially, the *in silico* structure-based protocols involving molecular docking method were internally validated by redocking the co-crystal ligand (Marcou and Rognan, 2007; Sevrioukova and Poulos, 2012). The valid protocols were subsequently employed to elucidate the binding mode of curcumin in the CYP3A4 active site. The visual inspection of the binding mode of curcumin identified the potential SOM of curcumin and lead to the prediction of the first possible metabolite of curcumin metabolism by CYP3A4.

METHODOLOGY

Materials

The crystal structure of human CYP3A4 bound to bromoergocryptine (BEC) obtained from protein data bank (PDB) with PDB code of 3UA1 was used as the reference structure (Sevrioukova and Poulos, 2012). The digital form of curcumin structure in the β-diketo tautomer was obtained from Chemical Entities of Biological Interest (ChEBI) database (https://www.ebi.ac.uk/chebi/init.do) with ChEBI-ID of CHEBI:3962 (European Bioinformatics Institute, 2012). The configurations for the docking simulations were provided by Yuniarti *et al.* (2011). All computational simulations were performed on a Hewlett-Packard™ HP 430 workstation with Intel® Core™ i3 as the processor and 2 GB of RAM and Linux 2.6.32-30-generic (Ubuntu 10.04 Lucid) as the operating system. Computational medicinal chemistry applications employed in this research were SPORES (ten Brink and Exner, 2009), PLANTS1.2 (Korb *et al*., 2009), Open Babel 2.2.3 (O'Boyle *et al*., 2011), PyPLIF 0.1.1 (Radifar, 2012), MarvinSketch 5.10.0 (ChemAxon, 2009) and PyMOL 1.2r1 (Lill and Danielson, 2011). Statistical analysis was performed by using R 2.14.0 (R Development Core Team, 2008).

Computational methods

Molecular docking protocols construction and internal validation

The virtual target file (protein.mol2) was prepared by employing the rule-based recognition of protonation, tautomeric, and stereoisomeric states of SPORES (ten Brink and Exner, 2009) subjected to the reference structure. The binding pocket of the human CYP3A4 was defined by the coordinates of the co-crystalized BEC in the 3UA1 structure (Sevrioukova and Poulos, 2012) and a radius of 14.401Å, which is the maximum distance from the center defined by a 5Å radius (de Graaf *et al.*, 2011) around BEC. Based on this binding pocket definition, the default configuration (Tabel I) was prepared according to the default configuration previously described by Yuniarti *et al.* (2011). In the visual inspection of the 3UA1 structure using PyMOL 1.2 (Lill and Danielson, 2011), several hydrogen bond interactions of BEC to the residues in the binding pocket, including the hydrogen bond interactions to SER119, ARG212, and THR224, were observed (Sevrioukova and Poulos, 2012). The hydrogen bond interaction of BEC to SER119 amongst other was observed as the nearest one (6.1Å) from the CYP3A4 heme Fe-atom (Sevrioukova and Poulos, 2012). Yuniarti *et al.* (2011) suggested a hydrogen bond anchor in order to increase the virtual screening quality. Therefore, beside the default molecular docking configuration, a modified configuration with 100 times hydrogen bonding constraint to SER119 was prepared (Table II).

The internal validations were performed for each configuration by redocking the co-crystalized ligand BEC into the virtual target using the docking software PLANTS1.2 (Korb *et al.*, 2009) and subsequently compared the docking pose to the original crystal structure pose (Marcou and Rognan, 2007; Sevrioukova and Poulos, 2012). The objective function used in the internal validation was the root mean square distance (RMSD) value between the heavy atoms of the docked pose and the crystal structure pose. A docking protocol is acceptable if the RMSD value is less than 2.0Å (Marcou and Rognan, 2007). The RMSD values were calculated using rms_cur module in PyMOL 1.2r1.

Ligand preparation steps

The optimized state of the lowest energy conformer of the co-crystalized ligand BEC was used as the input ligand. This optimized state was prepared by employing Open Babel 2.2.3 (O'Boyle *et al.*, 2011). The hydrogen atoms in pH 7.4 was added to the input ligand by module babel –p 7.4 and followed by module obconformer to perform conformer search using Monte Carlo simulations with maximum 250 conformers and followed by energy optimization using steepest descent method with maximum 100 steps. This ligand preparation step was performed 10 times to have 10 different starting points. Each prepared ligand were subsequently docked independently to the virtual target by employing PLANTS1.2 (Korb *et al.*, 2009). For each independent docking simulation, the best docked pose was automatically suggested by the software by selecting a pose with the lowest ChemPLP score.

Rescoring using protein-ligand interaction fingerprints calculated by PyPLIF

The docked poses resulted from the previous subsection were subjected to PyPLIF (Radifar, 2012) in order to calculate the protein-ligand interaction fingerprint (PLIF) bitstrings. The bitstrings were subsequently compared to the PLIF bitstrings of protein-ligand interactions of the crystal structure pose of ligand (BEC) to the defined binding pocket of the crystal structure of protein (3UA1) using Tanimoto similarity (Tc-PLIF) coefficient (Radifar, 2012). By using PyPLIF, the pose with the highest Tc-PLIF value was assigned as the selected pose instead of the pose with the lowest ChemPLP score.

Considering stereoisomer constraint in the ligand preparation step

The module obconformer in OpenBabel 2.2.3 could not provide the stereoisomer constraint (O'Boyle *et al.*, 2011). Therefore, beside the ligand preparation steps without stereoisomer constraint described in the previous sub section, other ligand preparation steps with the stereoisomer constraint were performed. Since the automatic option to constraint the stereoisomer was not available in

the module obconformer of OpenBabel 2.2.3 (O'Boyle *et al*., 2011), the stereoisomer of each prepared ligand was manually checked and the ligand preparation step was redone if the prepared ligand was not in the same stereoisomer state with the co-crystalized ligand BEC (Sevrioukova and Poulos, 2012). This ligand preparation step was performed several times until 10 different starting point ligands with the same stereoisomer state with the co-crystalized ligand BEC were available. Each prepared ligand were subsequently docked independently to the virtual target by employing PLANTS1.2 (Korb *et al*., 2009). The subsequent docking rescoring using PyPLIF 0.1.1 (Radifar, 2012) were also performed to the docked poses.

Docking simulation of curcumin

Curcumin in the β-diketo tautomer obtained from the ChEBI database was prepared using the previously described ligand preparation procedure. On the other hand, curcumin in the keto-enol tautomer was built in the two dimension (2D) form using MarvinSketch and using the module Major Microspecies the major microspecies in pH 7.4 was checked and subsequently the 10 different conformers were built using the default setting of the module Conformers. The 10 different conformers were then exported as a .mol2 file.

For each tautomer, 10 prepared ligands were provided independently as the starting points for the docking simulations. The best pose of curcumin in the binding pocket of human CYP3A4 from each tautomer was selected using the best and validated *in silico* screening protocol described in the previous subsections. This pose was subsequently inspected visually to study the SOM of curcumin by human CYP3A4. The SOM was the ligand atoms within 6.0 Å from the CYP3A4 heme Fe-atom (de Graaf *et al*., 2006). By identification of the SOM, the predicted metabolites can be subsequently suggested (de Graaf *et al*., 2005; Tamvakopoulos *et al*., 2007).

RESULTS AND DISCUSSION

This research was aimed to construct a valid *in silico* tool to study the human CYP3A4 enzyme-ligand interactions. In the context of an enzyme as catalytic receptor, the ligand can be a substrate or an inhibitor (de Graaf *et al*., 2005). The validated tool was subsequently employed to examine the interactions of curcumin to human CYP3A4 in the atomic level and identify its SOM (de Graaf *et al*., 2005, 2006, 2011).

Constraints are important to have a valid and acceptable in silico tool to study the human CYP3A4 enzyme-ligand interactions

A valid crystal structure-based *in silico* tool to study how a ligand, which was retrospectively proven to be active in a receptor, interacts to the receptor should have at least the ability to reproduce the original pose of the co-crystalized ligand (Marcou and Rognan, 2007). The pose produced and selected by a valid *in silico* tool must have an RMSD value of less than 2.0Å (Marcou and Rognan, 2007). The RMSD values of the best pose selected using the lowest ChemPLP score from 10 independent starting points (Conformers 1-10) without (the default configuration (Table I)) and with additional hydrogen bond interaction constraint to SER119 (the modified configuration (Table II)) are presented in table III, while table IV presents the RMSD values of the best pose selected using the highest Tc-PLIF value. Different to energy-based scoring functions used commonly in other docking softwares (Tiwari *et al*., 2009), ChemPLP score and Tc-PLIF are dimensionless since it is not an energy-based scoring functions. Instead, ChemPLP score is a knowledge-based empirical scoring functions (Korb *et al*., 2007, 2009), while Tc-PLIF is a similarity index comparing the PLIF bitstrings of the docked pose to the original co-crystalized pose (Marcou and Rognan, 2007). Therefore, it is not recommended to convert the scores to any affinity values. The ChemPLP score and the Tc-PLIF were employed to rank and assist the selection of the docked pose in a virtual screening campaign (Marcou and Rognan, 2007; de Graaf *et al*., 2011).

Based on table III and IV, none of these *in silico* protocols can be employed in the binding mode prediction of ligands when interact to the human CYP3A4.

Table I. The default configuration file of the molecular docking simulations by employing molecular docking software PLANTS1.2 used in this research.

Default Configuration
scoring function and search settings
scoring_function chemplp
search_speed speed1
input
protein_file ../protein.mol2
ligand_file ../01_ligand-preparation/ligand_input_all.mol2
output
output_dir redock_results
write single mol2 files (e.g., for RMSD calculation)
write_multi_mol2 0
cluster algorithm
cluster_structures 10
cluster_rmsd 2.0
binding site definition
bindingsite_center 22.7544 14.8129 -11.868
bindingsite_radius 14.401

Table II. The modified configuration file of the molecular docking simulations by employing molecular docking software PLANTS1.2 used in this research.

Modified Configuration
scoring function and search settings
scoring_function chemplp
search_speed speed1
input
protein_file ../protein.mol2
ligand_file ../01_ligand-preparation/ligand_input_all.mol2
output
output_dir redock_results
write single mol2 files (e.g., for RMSD calculation)
write_multi_mol2 0
cluster algorithm
cluster_structures 10
cluster_rmsd 2.0
binding site definition
bindingsite_center 22.7544 14.8129 -11.868
bindingsite_radius 14.401
hydrogen bond constraint
chemplp_protein_hb_constraint 1462 100

Table III. The ChemPLP scores and RMSD values of the best docked pose of BEC from 10 independent starting points selected based on the ChemPLP score.

Entry	Default Configuration		Modified Configuration	
	ChemPLP	RMSD (Å)	ChemPLP	RMSD (Å)
Conformer 1	-133.282	3.376	-408.453	1.420
Conformer 2	-137.117	3.476	-404.045	1.704
Conformer 3	-124.374	1.099	-418.036	1.087
Conformer 4	-130.179	3.550	-412.678	1.458
Conformer 5	-130.908	3.431	-408.118	1.632
Conformer 6	-131.322	1.416	-417.395	1.192
Conformer 7	-130.235	3.537	-415.795	1.347
Conformer 8	-126.439	0.903	-419.836	0.820
Conformer 9	-125.672	1.268	-416.786	0.921
Conformer 10	-120.002	9.159	-403.219	4.405

Table IV. The Tc-PLIF and RMSD values of the best docked pose of BEC from 10 independent starting points selected based on the Tc-PLIF value.

Entry	Default Configuration		Modified Configuration	
	Tc-PLIF	RMSD (Å)	Tc-PLIF	RMSD (Å)
Conformer 1	0.778	1.839	0.800	1.420
Conformer 2	0.833	1.966	0.750	1.704
Conformer 3	0.842	1.099	0.800	1.087
Conformer 4	0.895	1.521	0.800	1.458
Conformer 5	0.800	1.634	0.800	1.632
Conformer 6	0.850	1.294	0.842	1.192
Conformer 7	0.778	3.519	0.800	1.347
Conformer 8	0.833	0.903	0.842	0.820
Conformer 9	0.789	1.268	0.850	0.921
Conformer 10	0.650	4.751	0.714	5.457

Table V. The ChemPLP scores and RMSD values of the best docked pose of BEC from 10 independent stereoisomer-constrained starting points selected based on the ChemPLP score.

Entry	Default Configuration		Modified Configuration	
	ChemPLP	RMSD (Å)	ChemPLP	RMSD (Å)
Conformer 11	-127.846	3.547	-411.688	3.439
Conformer 12	-127.120	3.377	-409.126	1.237
Conformer 13	-127.000	3.424	-419.668	1.020
Conformer 14	-123.060	3.535	-416.071	1.125
Conformer 15	-132.340	3.390	-407.065	3.324
Conformer 16	-132.649	3.405	-409.930	3.365
Conformer 17	-125.128	0.968	-418.146	1.006
Conformer 18	-128.565	3.420	-402.132	1.654
Conformer 19	-128.915	3.566	-410.770	1.583
Conformer 20	-127.234	3.603	-409.585	1.614

Table VI. The Tc-PLIF and RMSD values of the best docked pose of BEC from 10 independent stereoisomer-constrained starting points selected based on the Tc-PLIF value.

Entry	Default Configuration		Modified Configuration	
	Tc-PLIF	RMSD (Å)	Tc-PLIF	RMSD (Å)
Conformer 11	0.947	1.614	0.800	1.733
Conformer 12	0.750	3.648	0.800	1.237
Conformer 13	0.789	1.557	0.800	1.020
Conformer 14	0.789	1.516	0.800	1.125
Conformer 15	0.750	1.966	0.800	1.604
Conformer 16	0.857	1.233	0.800	1.292
Conformer 17	0.778	3.678	0.750	1.006
Conformer 18	0.737	1.918	0.850	1.654
Conformer 19	0.800	1.573	0.800	1.583
Conformer 20	0.789	1.736	0.800	1.614

Table VII. The Tc-PLIF the best docked poses of curcumin in the β-diketo and keto-enol forms in the binding pocket of human CYP3A4 from 10 independent runs with different starting points.

Tc-PyPLIF	
Tautomers β-diketo	Tautomers Keto-enol
0.632	0.579
0.600	0.526
0.571	0.600
0.684	0.550
0.600	0.526
0.579	0.650
0.650	0.579
0.609	0.550
0.571	0.550
0.600	0.579

The default configuration without using PyPLIF (Table III) gave the worst results. Although the modified configuration (Table III) could reduce the RMSD values of 9 out of 10 conformers until less than 2.0Å, there were still possibilities of the ligand to be docked in the incorrect pose. Similar results to the use of modified configuration (Table III) were shown by the best poses selected by using the Tc-PLIF value. There was always one starting point (conformer 10) that gave RMSD value of more than 2.0Å. This outlier was then inspected visually and it was observed that conformer 10 had different stereoisomer compared to the reference co-crystalized ligand BEC and to other conformers. Thus, stereoisomer constraint in the ligand preparation step is highly recommended. The *in silico* construction and validation were then re-performed by taking into account this stereoisomer constraint issue.

Another 10 conformers (Conformers 11-20) were prepared independently and their stereoisomers were manually checked to make sure that the stereoisomer similar to the reference co-crystalized ligand BEC.

The RMSD values of the best pose selected using the lowest ChemPLP score from these 10 independent stereoisomer-constrained starting points without (the default configuration (Table I)) and with additional hydrogen bond interaction constraint to SER119 (the modified configuration (Table II)) are presented in table V, while table VI presents the RMSD values of the best pose selected using the highest Tc-PLIF value.

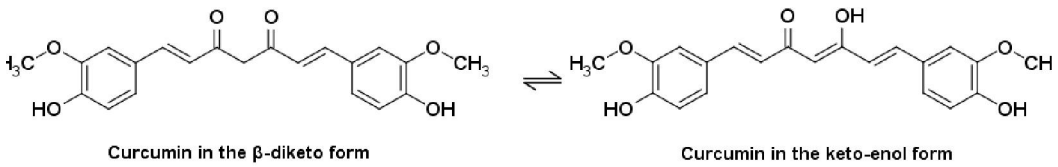

Figure 1. Structure of curcumin, both in the β-diketo and the keto-enol forms.

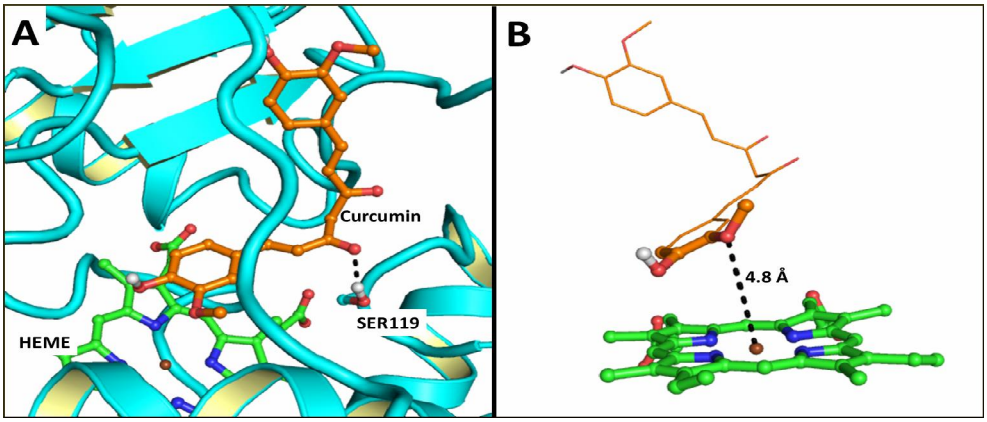

Figure 2. The representative pose of curcumin (orange carbon atoms) in the binding pocket of human CYP3A4 (blue carbon atoms except for heme using green carbon atoms). Oxygen, nitrogen and Fe are colored in red, blue and brown, respectively. Only polar hydrogens are shown for clarity. In 2A, curcumin is depicted as balls and sticks and only tertiary structure, SER119 and HEME of CYP3A4 are shown. Hydrogen bond interaction is depicted by black dashed line. In 2B, curcumin is depicted as lines except for atoms within 6.0 Å from the CYP3A4 heme Fe-atom, which are depicted as balls and sticks. Only curcumin and HEME are presented in 2B. The black dashed line in 2B represents the distance between the CYP3A4 heme Fe-atom and the most plausible SOM of curcumin.

As can be seen in table V and table VI, the use of hydrogen bond constraint to SER119 and PyPLIF rescoring were important to be involved in a valid *in silico* tool to predict the binding mode prediction of ligands when interact to the human CYP3A4. The default configuration alone could only give 1 acceptable RMSD value out of 10 independent simulations. The modified configuration or the use of PyPLIF could increase the quality but still some of the selected poses gave RMSD values more than 2.0Å. Only the ones that employing both modified configuration and PyPLIF rescoring gave RMSD values of less than 2.0Å. This indicates that interaction fingerprints with more attention to the ligand interaction to SER119 are important in the binding mode prediction of a ligand in the binding pocket of human CYP3A4. Notably, this successful *in silico* tool construction and validation was stereoisomer dependent. Therefore, in prospective efforts employing this validated tool should take into account the stereoisomer of the ligands in the preparation steps.

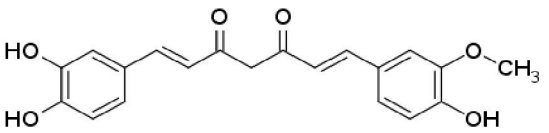

Figure 3. Structure of 1-(3,4-dihydroxy-phenyl)-5-hydroxy-7-(4-hydroxy-3-methoxy-phenyl) hepta-1,4,6-trien-3-one.

Curcumin binds to human CYP3A4 enzyme-ligand in the form of β-diketo tautomer

Since curcumin is a ligand for human CYP3A4 (Appiah-Opong, de Esch, *et al.*, 2008), we were confident to employ the previously validated *in silico* protocol, that can reproduce the pose of the co-crystal ligand (see previous subsection), to dock curcumin in and to analyze how curcumin binds in the binding pocket of CYP3A4. Curcumin can exist in two tautomers, *i.e.* β-diketo and keto-enol forms (Figure 1) (Istyastono *et al.*, 2003). Based on the existence of these tautomers and taking into account the stereoisomer dependency of the protocol, curcumin was analyzed here as both β-diketo and keto-enol tautomers. The results of 10 independent runs from 10 different starting points of each tautomer are presented in table VII.

Based on table VII, the statistical analysis of the Tc-PyPLIF values showed that curcumin is more likely in the β-diketo tautomer to bind to CYP3A4 than in the keto-enol tautomer. The Shapiro-Wilk test showed that the data is normal (p-value = 0.385). The Tc-PyPLIF values of the β-diketo and keto-enol tautomers are 0.610 ± 0.036 and 0.569 ± 0.037. The one-tailed t-test showed that the Tc-PyPLIF values of the β-diketo form are higher than the Tc-PyPLIF values of the keto-enol form significantly in the confidence level of 95% (p-value = 0.012). This indicates that the β-diketo form of curcumin is the more plausible tautomer than the keto-enol form of curcumin when binds to CYP3A4.

The first step metabolism of curcumin by CYP3A4 is O-demethylation

The representative figure depicted how curcumin binds to CYP3A4 in the binding pocket (Figure 2A) was prepared from the result of *in silico* screening with highest Tc-PYPLIF value (0.684). Figure 2B shows curcumin atoms within 6.0Å from the CYP3A4 heme Fe-atom which can be defined as the SOM of curcumin by CYP3A4 (Rendic, 2002; de Graaf *et al.*, 2006). The most frequent reaction catalyzed by CYP3A4 is O-dealkylation (Rendic, 2002). Based on Figure 2B, there is a moiety in curcumin within 6.0Å from the CYP3A4 heme Fe-atom that can be metabolized by O-dealkylation reaction, *i.e.* O-methoxy moiety. Therefore, the first reaction metabolism by CYP3A4 of curcumin is O-demethylation with an oxidative metabolite 1-(3,4-dihydroxyphenyl)-5-hydroxy-7-(4-hydroxy-3-methoxy-phenyl)hepta-1,4,6-trien-3-one (Fig.3) as the first plausible metabolite. This confirms the newly identified curcumin metabolites by Tamvakopoulos *et al.* (2007). Together with the results presented by Tamvakopoulos *et al.* (2007), these *in silico* screening results suggest that curcumin is not only a ligand nor an inhibitor to human CYP3A4 (Appiah-Opong *et al.*, 2009), but also a substrate metabolized by the enzyme to an oxidative metabolite 1-(3,4-dihydroxyphenyl)-5-hydroxy-7-(4-hydroxy-3-methoxyphenyl)hepta-1,4,6-trien-3-one. In contrary, some *in vitro* and *in vivo* studies (which mostly employing animal models) performed previously stated that no oxidative metabolite of curcumin was observed (Asai and Miyazawa, 2000; Ireson *et al.*, 2001; Hoehle *et al.*, 2006; Anand *et al.*, 2007). These recent findings of the trace of oxidative metabolites of curcumin (Tamvakopoulos *et al.*, 2007) and the mechanism of oxidative metabolites formation of curcumin in the atomic level (presented in this article) open new insight of the curcumin metabolism by human CYP450, especially by CYP3A4.

CONCLUSIONS

The validated *in silico* protocols to identify ligands for human CYP3A4 can successfully identify the more plausible tautomeric form of curcumin when binds to human CYP3A4. Employing the best pose of curcumin in the binding pocket of human CYP3A4 selected by protocols and using the criteria proposed by de Graaf *et al.* (de Graaf *et al.*, 2006), the first oxidative product of curcumin metabolism by human CYP3A4, 1-(3,4-dihydroxyphenyl)-5-hydroxy-7-(4-hydroxy-3-methoxy-phenyl)hepta-1,4,6-trien-3-one, can be identified.

ACKNOWLEDGEMENT

This work was supported by Indonesian Toray Science Foundation, through the Science and Technology Research Grant 2011.

REFERENCES

Anand P., Kunnumakkara AB., Newman RA., and Aggarwal, B.B., 2007, Bioavailability of curcumin: Problems and promises, *Mol. Pharmaceutics*, 4, 807-818.

Appiah-Opong R., Commandeur JNM., Axson C., and Vermeulen, NPE., 2008, Interactions between cytochromes P450, glutathione S-transferases and Ghanaian medicinal plants, *Food Chem. Toxicol.*, 46, 3598-3603.

Appiah-Opong R., Commandeur JNM., Istyastono E., Bogaards JJ., and Vermeulen NPE., 2009, Inhibition of human glutathione S-transferases by curcumin and analogues, *Xenobiotica*, 39, 302-311.

Appiah-Opong R., Commandeur JNM., van Vugt-Lussenburg, B., and Vermeulen, N.P.E., 2007, Inhibition of human recombinant cytochrome P450s by curcumin and curcumin decomposition products, *Toxicology*, 235, 83-91.

Appiah-Opong R., de Esch I., Commandeur, J.N.M., Andarini, M., and Vermeulen, N.P.E., 2008. Structure-activity relationships for the inhibition of recombinant human cytochromes P450 by curcumin analogues, *Eur. J. Med. Chem.*, 43, 1621-1631.

Asai A. and Miyazawa T., 2000, Occurrence of orally administered curcuminoid as glucuronide and glucuronide/sulfate conjugates in rat plasma, *Life Sci.*, 67, 2785-2793.

Basnet P. and Skalko-Basnet N., 2011, Curcumin: An anti-inflammatory molecule from a curry spice on the path to cancer treatment, *Molecules*, 16, 4567-4598.

ChemAxon, 2009. *Marvin Beans 5.2.5.1* (http://www.chemaxon.com/products/marvin/), Budapest.

de Graaf C., Kooistra AJ., Vischer HF., Katritch V., Kuijer M., Shiroishi M., Iwata S., Shimamura T., Stevens RC., de Esch IJP., and Leurs R., 2011, Crystal structure-based virtual screening for fragment-like ligands of the human histamine H_1 receptor, *J. Med. Chem.*, 54, 8195-8206.

de Graaf C., Oostenbrink C., Keizers PHJ., van der Wijst T., Jongejan A., and Vermeulen NPE., 2006, Catalytic site prediction and virtual screening of cytochrome P450 2D6 substrates by consideration of water and rescoring in automated docking, *J. Med. Chem.*, 49, 2417-2430.

de Graaf C., Vermeulen NPE., and Feenstra, K.A., 2005, Cytochrome p450 in silico: An integrative modeling approach, *J. Med. Chem.*, 48, 2725-2755.

European Bioinformatics Institute, 2012. *ChEBI, 2010* (https://www.ebi.ac.uk/chebi/init.do. Accessed 1 September 2012), Cambridgeshire..

Hoehle SI., Pfeiffer E., Sólyom AM., and Metzler M., 2006, Metabolism of curcuminoids in tissue slices and subcellular fractions from rat liver, J. Agri. Food Chem., 54, 756-764.

Ireson C., Orr S., Jones DJL., Verschoyle R., Lim C., Luo J., Howells L., Plummer S., Jukes R., Williams M., Steward WP., and Gescher A., 2001, Characterization of metabolites of the chemopreventive agent curcumin in human and rat hepatocytes and in the rat *in vivo* , and evaluation of their ability to inhibit phorbol ester-induced prostaglandin E_2 production, *Cancer Res.*, 61, 1058-1064.

Istyastono EP., Supardjan, and Pranowo HD., 2003, Tautomeri Keto-Enol Kurkumin dan Beberapa Turunan Kurkumin Tersubstitusi pada C-4 : Suatu Kajian Teoritis Berdasarkan Pendekatan Kimia Komputasi, *Indo. J. Chem.*, 14, 107-113.

Komura H. and Iwaki M., 2011, *In vitro* and *in vivo* small intestinal metabolism of CYP3A and UGT substrates in preclinical animals species and humans: Species differences, *Drug Metab. Rev.*, 43, 476-498.

Korb O., Stützle T., and Exner TE., 2007, An ant colony optimization approach to flexible protein–ligand docking, *Swarm Intelligence,* 1, 115-134.

Korb O., Stützle T., and Exner TE., 2009. Empirical scoring functions for advanced protein-ligand docking with PLANTS, *J. Chem. Inf. Model.*, 49, 84-96.

Kunwar A., Barik A., Mishra B., Rathinasamy K., Pandey R., and Priyadarsini KI., 2008, Quantitative cellular uptake, localization and cytotoxicity of curcumin in normal and tumor cells, *BBA*, 1780, 673-679.

Lill MA. and Danielson ML., 2011, Computer-aided drug design platform using PyMOL, *J. Comput.-Aided Mol. Des.*, 25, 13-19.

Marcou G. and Rognan D., 2007, Optimizing fragment and scaffold docking by use of molecular interaction fingerprints, *J. Chem. Inf. Model.*, 47, 195-207.

O'Boyle NM., Banck M., James CA., Morley C., Vandermeersch T., and Hutchison G.R., 2011, Open Babel: An open chemical toolbox, *J.Cheminform.*, 3, 33-46.

R Development Core Team, 2008, *R: A Language and Environment for Statistical Computing* (http://www.r-project.org), Vienna.

Radifar M., 2012. *PyPLIF 0.1.1* (http://code.google.com/p/pyplif/ Accessed 31 August 2012).

Rendic S., 2002, Summary of information on human CYP enzymes: human P450 metabolism data, *Drug Metab. Rev.*, 34, 83-448.

Sevrioukova IF. and Poulos TL., 2012, Structural and mechanistic insights into the interaction of cytochrome P450 3A4 with bromoergocryptine, a type I ligand. *J. Biol. Chem.*, 287, 3510-3517.

Tamvakopoulos C., Sofianos ZD., Garbis SD., and Pantazis, P., 2007, Analysis of the in vitro metabolites of diferuloylmethane (curcumin) by liquid chromatography--tandem mass spectrometry on a hybrid quadrupole linear ion trap system: Newly identified metabolites, *Eur. J. Drug Metab. Pharmacokinet.*, 32, 51-57.

ten Brink T. and Exner TE., 2009, Influence of protonation, tautomeric, and stereoisomeric states on protein-ligand docking results, *J. Chem. Inf. Model.*, 49, 1535-1546.

Tiwari R., Mahasenan K., Pavlovicz R., Li, C., and Tjarks W., 2009, Carborane clusters in computational drug design: A comparative docking evaluation using AutoDock, FlexX, Glide, and Surflex, *J. Chem. Inf. Model.*, 49, 1581-1589.

Yuniarti N., Ikawati Z., and Istyastono EP., 2011, The importance of ARG513 as a hydrogen bond anchor to discover COX-2 inhibitors in a virtual screening campaign, *Bioinformation*, 6, 164-166.